

Few-Nucleon Systems: Notes about the Status and Results of Investigations

Yu.P.Lyakhno

April 3, 2024

*National Science Center "Kharkov Institute of Physics and Technology"
61108, Kharkiv, Ukraine*

Abstract

The model-independent calculation of the nuclei ground state and the states of scattering can be carried out with due regard for realistic NN and $3N$ forces between nucleons and also, with the use of exact methods of solving the many-nucleon problem. The tensor part of NN interaction and $3NF$'s generate the lightest nuclei states with nonzero orbital momenta of nucleons. These states in the lightest nuclei are the manifestation of the properties of inter-nucleonic forces, and therefore, similar effects should be observed in all nuclei and also in all their excited states. In this paper primary attention is given to the investigation of the ${}^4\text{He}$ nucleus.

PACS numbers: 21.30.-x; 21.45.+v; 25.20.-x; 27.90.+b.

1 Introduction

From the physical standpoint, to describe the nucleon system, one must know the nucleon properties and inter-nucleonic forces. The world constants and nucleon properties are known within sufficient accuracy, while inter-nucleonic forces are complicated in character and are known to a less accuracy. Unlike the atom, these forces cannot be described by the $1/r^2$ ratio (where r is the distance between nucleons) or by more complicated expressions like the Woods-Saxon potential [1]. The distinctive feature of inter-nucleonic forces is that they depend not only on the distance r , but also on the quantum configuration of the nucleon system, which is determined by the orbital momentum L , spin S and isospin T of this system.

The NN potential can be determined phenomenologically from the experimental data on the ground state of the two-nucleon system and on the elastic (p,p) , (n,p) and (n,n) scattering at nucleon energies up to 500 MeV. At higher nucleon energies, nonelastic processes come into play, and the potential approach becomes inapplicable. However, the data about the inter-nucleonic forces in this nucleon energy region are sufficient for the description of nucleus ground state, and also of nuclear reactions up to the meson-producing threshold. Nowadays, Argonne AV18 [2] and CD-Bonn [3] appear to be the most accurate potentials. In the construction of the charge-dependent CD-Bonn potential in the range of laboratory-system nucleon energies up to 350 MeV, 2932 (p,p) - and 3058 (n,p) - scattering data were used. Adjustable expressions were

derived on the basis of the meson model of strong interaction of nucleons. Into the account were taken the π , η , ρ , ω -one-meson-exchange contribution, σ - one-boson-exchange, 2π -exchange, including Δ -isobar configurations, and of the $\pi\rho$ -exchange contribution. The calculations of the NN potential waves were up to $J \leq 4$ (the following notation is used for the purpose: $^{2S+1}L_J$, J is the total momentum of the system). The quantity χ^2/datum was found to be 1.02.

Mathematically, to describe the nucleon system, it is necessary to use the accurate methods of solving the many-nucleon problem. To describe the three-body system in the case of an arbitrary two-body potential, Faddeev [4] suggested solving a set of connected integral equations. Later on, Yakubovsky [5] generalized this result for the case of any number of particles in the system. At present, it is found that $3N$ forces take action in the nucleus. In the calculations, the $3N$ potentials of types UrbanaIX [6] and Tucson-Melbourne [7, 8] are most frequently used. So, for exact description of a many-nucleon system it is necessary to solve the set of connected integral equations with due regard for the contribution of NN and $3N$ forces. The solution of the problem by the Faddeev-Yakubovsky (FY) method was reported by Gloeckle and Kamada (GK) [9]. The characteristics of ground states three- and four-nucleon nucleus by the FYGK method were calculated in papers [10]-[14].

The realistic NN and NNN forces were also used in the calculations by the Lorentz integral transform (LIT) method [15], the hyperspherical harmonic variational method (HHVM) [16], the refined resonating group model (RRGM) [17] and others [18].

It is hoped that the accuracy of measurements of realistic NN and NNN potentials would get further better, in particular, at the expense of using the data from double-polarization experiments [19]. A number of laboratories create targets of the polarized ^3He nuclei [20]-[22]. The investigation of disintegration of polarized ^3He nuclei by polarized beams of particles can provide some new information about $3N$ forces.

Along with the elaboration more precise definition of phenomenological potentials, important results were obtained through theoretical calculations of inter-nucleonic forces within the framework of chiral effective field theory (EFT). At present, the calculation of chiral interactions is not as accurate as that of phenomenological NN forces. Calculated within the framework of the EFT, the NN potential parameters for partial waves with $J \leq 2$ [23] are in satisfactory agreement with the experiment in the region of nucleon lab energy up to $T_N \sim 290$ MeV. In the context of the EFT, Rozpedzik *et al.* [24] estimated the effect of $4N$ forces and found the additional contribution of $4N$ forces to the binding energy of the ^4He nucleus to be about several hundreds of keV. The calculations in the context of EFT are of particular importance for explaining the origin and explicit representation of $3N$ and $4N$ forces. The reason is that there are a good many experimental data to determine the NN potential, whereas for determination of $3N$ and $4N$ forces these data are not nearly enough. The origin and the explicit form of $3N$ and $4N$ forces is a basic issue of few-nucleon systems.

Section 2 presents the results of theoretical calculations of the ground states of few-nucleon nuclei. Section 3 presents the multipole analysis of the $^4\text{He}(\gamma, p)\text{T}$ and $^4\text{He}(\gamma, n)^3\text{He}$ reactions, performed on the basis of the experimental data about the differential cross-sections and cross-section asymmetry with linearly polarized photons. The possible effects, determined by realistic inter-nucleonic forces in nuclei with $A > 4$ are discussed in Section 4. The conclusions are formulated in Section 5.

2 Results of the theoretical calculations

In Ref.[11] calculation of the ground-state of the α -particle is carried out. The calculations took into account the contributions from the states of the NN system having the total momentum up to $J \leq 6$. The consideration of large total-momentum values of the two-nucleon system is necessary, for example, for a correct calculation of short-range correlations. In the calculation [11], account was taken of the states, in which the algebraic sum of orbital momenta of all nucleons of the ${}^4\text{He}$ nucleus was no more than $l_{max}=14$. The system comprised 6200 partial waves. The authors of work [11] estimated their mistake in the calculations of ${}^4\text{He}$ nuclear binding energy to be ~ 50 keV. Considering that the calculated value of the binding energy is ~ 200 keV higher than the experimental value, the authors have made a conclusion about a possible contribution of $4N$ forces that are of repulsive nature.

Table 1 lists the values of nuclear binding energies (in MeV) for ${}^4\text{He}$, ${}^3\text{H}$, ${}^3\text{He}$ and ${}^2\text{H}$, calculated with the use of NN potentials AV18 and $3NF$'s UrbanaIX. It is evident from the table that without taking into account the $3N$ forces, the nuclei appear underbound, while with due regard for the forces the agreement with experimental data is satisfactory.

T a b l e 1: Binding energies (in MeV units) of ${}^4\text{He}$, of ${}^3\text{H}$, of ${}^3\text{He}$ and of ${}^2\text{H}$, calculated with Argonne V18 and Argonne V18 + Urbana IX interaction.

Inter-action	Method	${}^4\text{He}$	${}^3\text{H}$	${}^3\text{He}$	${}^2\text{H}$
AV18	FY	-24.28	-7.628	-6.924	
	RRGM	-24.117	-7.572	-6.857	-2.214
	HHVM	-24.25			
AV18+ +UIX	FY GK	-28.50	-8.48	-7.76	
	RRGM	-28.342	-8.46	-7.713	-2.214
	HHVM	-28.50	-8.485	-7.742	
	Exp	-28.296	-8.481	-7.718	-2.224

Similar results were obtained with the use of the NN potential CD-Bonn and the $3N$ potential Tucson-Melbourne.

Table 2 gives the calculated root-mean-square radii r_{rms} of the ${}^4\text{He}$ nucleus [16, 17]. The agreement with experiment is also satisfactory.

T a b l e 2: The ${}^4\text{He}$ nucleus $\langle r^2 \rangle^{1/2}$ radii (fm).

Interaction	Method	${}^4\text{He}$
AV18	RRGM	1.52
	HHVM	1.512
AV18+UIX	RRGM	1.44
	HHVM	1.43
	Exp	1.67

It should be also noted that the Coulomb interaction between protons results in the production of $T=1$ and $T=2$ isospin states of ${}^4\text{He}$. Table 3 gives the probabilities of these states for the ${}^4\text{He}$ nucleus calculated in papers [11], [16].

T a b l e 3: Contribution of different total isospin states to the ^4He nuclear wave function. The values are given in %.

Interaction	Method	T=0	T=1	T=2
AV18	FY	99.992	$3 \cdot 10^{-3}$	$5 \cdot 10^{-3}$
	HHVM		$2.8 \cdot 10^{-3}$	$5.2 \cdot 10^{-3}$

The tensor part of NN interaction and $3NF$'s generate the ^4He nuclear states with nonzero orbital momenta of nucleons. Table 4 gives the probabilities of S , S' , P and D states of the ^4He and ^3He nuclei calculated by Nogga *et al.* [11], where S' is a part of 1S_0 -states with nonzero orbital momenta of nucleons. The calculations gave the probability of 5D_0 states having the total spin $S=2$ and the total nucleon orbital momentum $L=2$ of the ^4He nucleus to be $\sim 16\%$, and the probability of 3P_0 states having $S=1$, $L=1$ to be between 0.6% and 0.8%. It is obvious from Table 4 that the consideration of the $3NF$'s contribution increases the probability of 3P_0 states by a factor of ~ 2 .

T a b l e 4: S , S' , P , and D state probabilities for ^4He and ^3He .

Interaction	^4He				^3He			
	$S\%$	$S'\%$	$P\%$	$D\%$	$S\%$	$S'\%$	$P\%$	$D\%$
AV18	85.45	0.44	0.36	13.74	89.95	1.52	0.06	8.46
CD-Bonn	88.54	0.50	0.23	10.73	91.45	1.53	0.05	6.98
AV18+UIX	82.93	0.28	0.75	16.04	89.39	1.23	0.13	9.25
CD-Bonn+TM	89.23	0.43	0.45	9.89	91.57	1.40	0.10	6.93

3 The multipole analysis of $^4\text{He}(\gamma, p)^3\text{H}$ and $^4\text{He}(\gamma, n)^3\text{He}$ reactions

In the $E1$, $E2$ and $M1$ approximations, the laws of conservation of the total momentum and parity for two-body (γ, p) and (γ, n) reactions of ^4He nuclear disintegration permit two multipole transitions $E1^1P_1$ and $E2^1D_2$ with the spin $S=0$ and four transitions $E1^3P_1$, $E2^3D_2$, $M1^3S_1$ and $M1^3D_1$ with the spin $S=1$ of final-state particles. The differential cross section in the c.m.s. can be expressed in terms of multipole amplitudes as follows [25, 26]:

$$\begin{aligned}
\frac{d\sigma}{d\Omega} = & \frac{\lambda^2}{32} \{ \sin^2 \theta [18 |E1^1 P_1|^2 - 9 |E1^3 P_1|^2 \\
& + 9 |M1^3 D_1|^2 - 25 |E2^3 D_2|^2 \\
& - 18\sqrt{2} \text{Re}(M1^3 S_1^* M1^3 D_1) + 30\sqrt{3} \text{Re}(M1^3 D_1^* E2^3 D_2) \\
& + 30\sqrt{6} \text{Re}(M1^3 S_1^* E2^3 D_2) \\
& + \cos \theta (60\sqrt{3} \text{Re}(E1^1 P_1^* E2^1 D_2) \\
& - 60 \text{Re}(E1^3 P_1^* E2^3 D_2)) \\
& + \cos^2 \theta (150 |E2^1 D_2|^2 - 100 |E2^3 D_2|^2) \\
& + \cos \theta [-12\sqrt{6} \text{Re}(E1^3 P_1^* M1^3 S_1) \\
& - 12\sqrt{3} \text{Re}(E1^3 P_1^* M1^3 D_1) + 60 \text{Re}(E1^3 P_1^* E2^3 D_2)] \\
& + 18 |E1^3 P_1|^2 + 12 |M1^3 S_1|^2 + 6 |M1^3 D_1|^2 \\
& + 50 |E2^3 D_2|^2 + 12\sqrt{2} \text{Re}(M1^3 S_1^* M1^3 D_1) \\
& - 20\sqrt{6} \text{Re}(M1^3 S_1^* E2^3 D_2) - 20\sqrt{3} \text{Re}(M1^3 D_1^* E2^3 D_2) \} ,
\end{aligned} \tag{1}$$

where λ is the reduced wavelength of the photon.

It is known that the cross-section asymmetry of the linearly polarized photon reaction is described by the following expression [27]:

$$\begin{aligned}
\Sigma(\theta) = & \sin^2 \theta \{ 18 |E1^1 P_1|^2 - 9 |E1^3 P_1|^2 \\
& - 9 |M1^3 D_1|^2 + 25 |E2^3 D_2|^2 \\
& + 18\sqrt{2} \text{Re}(M1^3 S_1^* M1^3 D_1) + 10\sqrt{3} \text{Re}(M1^3 D_1^* E2^3 D_2) \\
& + 10\sqrt{6} \text{Re}(M1^3 S_1^* E2^3 D_2) \\
& + \cos \theta [60\sqrt{3} \text{Re}(E1^1 P_1^* E2^1 D_2) \\
& - 60 \text{Re}(E1^3 P_1^* E2^3 D_2)] \\
& + \cos^2 \theta [150 |E2^1 D_2|^2 - 100 |E2^3 D_2|^2] \} / \frac{32}{\lambda^2} \frac{d\sigma}{d\Omega} .
\end{aligned} \tag{2}$$

The differential cross section can be presented as:

$$\frac{d\sigma}{d\Omega} = A [\sin^2 \theta (1 + \beta \cos \theta + \gamma \cos^2 \theta) + \varepsilon \cos \theta + \nu] . \tag{3}$$

In the same terms, the cross-section asymmetry of the linearly polarized photon reaction can be represented as follows:

$$\Sigma(\theta) = \frac{\sin^2 \theta (1 + \alpha + \beta \cos \theta + \gamma \cos^2 \theta)}{\sin^2 \theta (1 + \beta \cos \theta + \gamma \cos^2 \theta) + \varepsilon \cos \theta + \nu} . \tag{4}$$

The coefficients A , α , β , γ , ε , and ν are unambiguously connected with multipole amplitudes. As it is obvious from relation (3), only 5 independent coefficients can be calculated in the long-wave approximation using the data on the differential reaction cross-section. So, an improvement in the accuracy of measuring only the differential reaction cross-section gives no way of obtaining information about subsequent multipole amplitudes. In this case, the number of unknown parameters in the right side of eq. (1) would increase much quicker than the

number of found coefficients in the left side of the equation. In this connection, in order to obtain information on the succeeding multipole amplitudes, polarization experiments or other data sources are required. As it can be seen from relation (4), the experimental data on the asymmetry of the linearly polarized photon reaction cross-section enable one to calculate the sixth independent coefficient.

It can be demonstrated that on the assumption that $\sigma(E2^3D_2) \gg \sigma(M1)$, from expressions (1) and (2) we obtain:

$$\alpha = \frac{50|E2^3D_2|^2}{18|E1^1P_1|^2 - 9|E1^3P_1|^2 - 25|E2^3D_2|^2} > 0. \quad (5)$$

If we assume that $\sigma(M1) \gg \sigma(E2^3D_2)$, then we have

$$\begin{aligned} \alpha = & \{-18|M1^3D_1|^2 \\ & + 36\sqrt{2}|M1^3S_1||M1^3D_1|\cos[\delta(^3S_1) - \delta(^3D_1)]\} / \\ & \{18|E1^1P_1|^2 - 9|E1^3P_1|^2 + 9|M1^3D_1|^2 \\ & - 18\sqrt{2}|M1^3S_1||M1^3D_1|\cos[\delta(^3S_1) - \delta(^3D_1)]\}. \end{aligned} \quad (6)$$

From the phase analysis of elastic (p, ^3He) scattering Murdoch *et al.* [28] have determined the phase difference to be $\delta(^3S_1) - \delta(^3D_1) > 90^\circ$. Therefore, the both components in the numerator of expression (6) enter with the minus sign, and the coefficient α must be negative.

The angular dependence of cross-section asymmetry in the $^4\text{He}(\vec{\gamma}, p)\text{T}$ and $^4\text{He}(\vec{\gamma}, n)^3\text{He}$ reactions with linearly polarized photons of energies 40, 56 and 78 MeV was measured by Lyakhno *et al.* [27, 29]. The beam of linearly polarized photons was produced as a result of coherent bremsstrahlung of 500, 600 and 800 MeV electrons, respectively, in a thin diamond single crystal. The reaction products were registered with the use of a streamer chamber located in the magnetic field [30]. The observed data on the angular dependence of the cross-section asymmetry are presented in Fig.1. Here the square represents the data obtained with semiconductor detectors by the ΔE -E method [31]. The dashed curve is the calculation by Mel'nik and Shebeko [32] made in the plane-wave impulse approximation with consideration of the direct reaction mechanism and the mechanism of recoil. The solid curves represent the calculation [33] that meets the requirements of covariance and gauge invariance. The calculation took into account the contribution of a number of diagrams corresponding to the pole mechanisms in s-, t- and u-channels, the contact diagram c, and also a number of triangular diagrams. A satisfactory fit of the calculation to the experiment confirms an essential role of the direct reaction mechanism, the mechanism of recoil and the final-state rescattering effects.

As a result of the least-squares fit of expressions (3) and (4) to the experimental data on the differential cross section [34, 35] and cross-section asymmetry of linearly polarized photon reactions, the coefficients A , α , β , γ , ε , and ν were calculated [27]. Since the coefficients enter into relations (3) and (4) in linear fashion, the solution was unambiguous.

Since only phase differences enter into formulas (1) and (2), these relations comprise 11 unknown parameters. The currently available experimental data on the (γ, p) and (γ, n) reactions are insufficient for determining all the parameters. According to the experimental data obtained (see Fig.2), α_p and α_n are the minus coefficients, and hence, the least amplitude that enters into expressions (1) and (2) is the $E2^3D_2$ amplitude. After the $E2^3D_2$ -comprising components are excluded, expressions (1) and (2) still comprise 9 unknown parameters: $|E1^1P_1|$, $|E2^1D_2|$, $\cos[\delta(^1P_1) - \delta(^1D_2)]$, $|E1^3P_1|$, $|M1^3S_1|$, $|M1^3D_1|$, $\cos[\delta(^3S_1) - \delta(^3D_1)]$, $\cos[\delta(^3S_1) - \delta(^3P_1)]$ and $\cos[\delta(^3P_1) - \delta(^3D_1)]$.

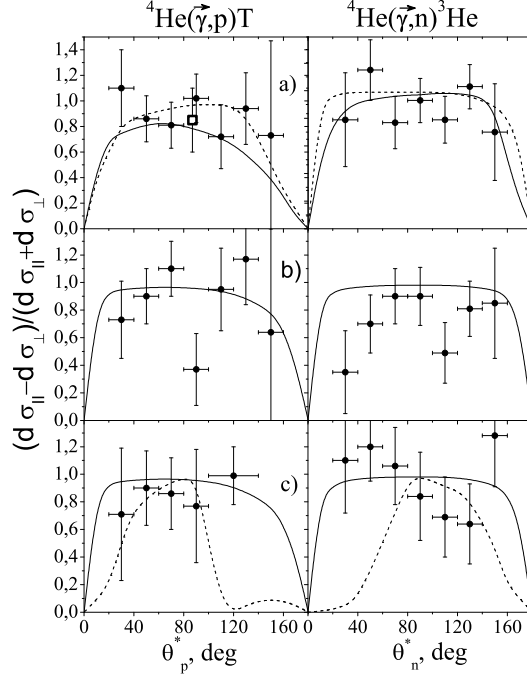


Figure 1: Angular dependence of cross-section asymmetry ${}^4\text{He}(\vec{\gamma}, p){}^3\text{H}$ and ${}^4\text{He}(\vec{\gamma}, n){}^3\text{He}$ reactions with linearly polarized photon. The points represent the results of Refs. [27, 29]: a) $E_{\gamma}^{peak}=40$ MeV, b) $E_{\gamma}^{peak}=56$ MeV, c) $E_{\gamma}^{peak}=78$ MeV. The square shows the data of Ref. [31]. The errors are statistical. The solid curve - from Ref. [33], the dashed curve - from Ref. [32].

It is known [36] that according to the isospin selection rules for self-conjugate nuclei the isoscalar parts of $E1$ and $M1$ amplitudes are essentially suppressed. In view of this, using the Watson theorem, the last three phase differences were calculated from the data of phase analysis of elastic $(p, {}^3\text{He})$ scattering [28].

The coefficients A , α , β , γ , ε , and ν are expressed in terms of the multipole amplitudes as:

$$A = \lambda^2/32\{18|E1^1P_1|^2 - 9|E1^3P_1|^2 + 9|M1^3D_1|^2 - 18\sqrt{2}|M1^3S_1||M1^3D_1|\cos[\delta(^3S_1) - \delta(^3D_1)]\}; \quad (7)$$

$$\alpha = \{-18|M1^3D_1|^2 + 36\sqrt{2}|M1^3S_1||M1^3D_1|\cos[\delta(^3S_1) - \delta(^3D_1)]\} / \frac{32}{\lambda^2}A; \quad (8)$$

$$\beta = 60\sqrt{3}|E1^1P_1||E2^1D_2|\cos[\delta(^1P_1) - \delta(^1D_2)] / \frac{32}{\lambda^2}A; \quad (9)$$

$$\gamma = 150|E2^1D_2|^2 / \frac{32}{\lambda^2}A; \quad (10)$$

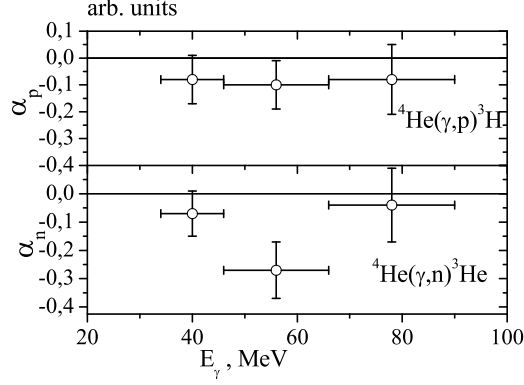


Figure 2: Coefficients α_p and α_n . The errors are statistical only.

$$\varepsilon = \{-12\sqrt{3}|E1^3P_1||M1^3D_1| \cos[\delta(^3P_1) - \delta(^3D_1)] - 12\sqrt{6}|E1^3P_1||M1^3S_1| \cos[\delta(^3P_1) - \delta(^3S_1)]\} / \frac{32}{\lambda^2} A; \quad (11)$$

$$\nu = \{18|E1^3P_1|^2 + 12|M1^3S_1|^2 + 6|M1^3D_1|^2 + 12\sqrt{2}|M1^3S_1||M1^3D_1| \cos[\delta(^3S_1) - \delta(^3D_1)]\} / \frac{32}{\lambda^2} A. \quad (12)$$

The experimentally observable quantities are expressed in terms of multipole amplitudes in a bilinear fashion. Therefore, there must exist two different sets of multipole amplitudes, which satisfy these experimental data. With the help of programs of the least square method (LSM) one positive solution of the problem can be calculated. The second solution can be found, for example, by the lattice method. Since both positive solutions have the equal χ^2 values, an additional information is necessary to choose the proper solution. It should be also noted that if the difference between the solutions is comparable with the amplitude errors, then the LSM errors of the amplitudes may appear overestimated.

The amplitude values were calculated from the derived set of six bilinear equations (7-12) with six unknown parameters using the random-test method [27]. To calculate the errors in the amplitudes, 5000 statistical samplings of A , α , β , γ , ε , and ν values with their errors were performed. The errors in the coefficients were assumed to be distributed by the normal law. After each statistical sampling the set of equations was solved, the calculated amplitude values were stored and then their average values and dispersions were calculated.

According to Ref. [37], one can assume that with the photon energy increase the $M1^3S_1$ transition cross-section decreases as $1/V$, where V is the nucleon velocity. Therefore, at MeV nucleon energies the contribution of the $M1^3S_1$ transition can be neglected. In this connection, out of the two found solutions of the system of equations (7-12) the choice has been made on the solution, where $\sigma(E1^3P_1) > \sigma(M1^3S_1)$.

The findings of the experiment aimed to determine the total cross sections of $S=1$ tran-

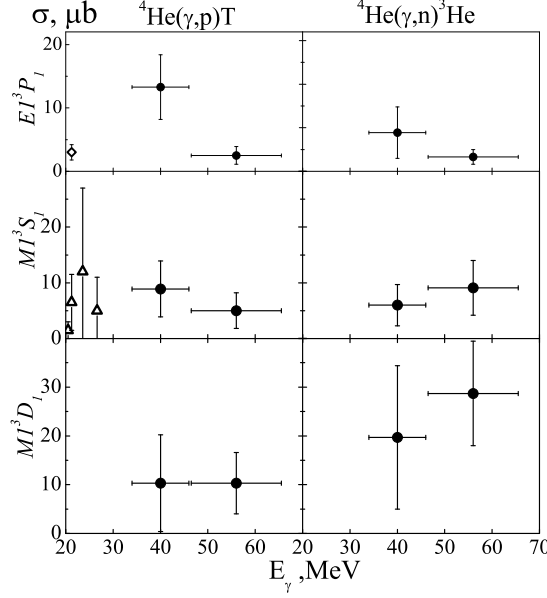


Figure 3: Total cross sections of spin $S=1$ transitions of ${}^4\text{He}(\gamma, p){}^3\text{H}$ and ${}^4\text{He}(\gamma, n){}^3\text{He}$ reactions: \diamond -data from Ref. [37]; \triangle -data of Ref. [38]; \bullet -data of Ref. [27]. The errors are statistical only.

sitions are presented in Fig.3. The triangles represent the data of Wagenaar *et al.* [38], the diamond shows the data of Pitts [37] obtained from studies of the reaction of radiative capture of protons by tritium nuclei. The points represent the data of Lyakhno *et al.* [27] from the studies of two-body (γ, p) and (γ, n) reactions of ${}^4\text{He}$ disintegration. The existing experimental data on the total cross-sections of electromagnetic transitions with the spin $S=1$ in the ${}^4\text{He}(\gamma, p)\text{T}$ and ${}^4\text{He}(\gamma, n){}^3\text{He}$ reactions have considerable statistic and systematic errors.

4 Role of the spin-orbit interaction in nuclei

The occurrence of states with nonzero orbital momenta of nucleons in the lightest nuclei is a manifestation of the properties of inter-nucleonic forces and, hence, such effects should be observed without exception in all nuclei as well as in all their excited states.

One can suppose that the contribution of the effects connected with the tensor part of NN potential and $3NF$'s increases with a growth of the atomic number. Firstly, it can be seen from the fact that the D -state contribution in the deuteron is about 5%, while in the ${}^4\text{He}$ nucleus it makes $\sim 16\%$.

Secondly, at the calculation of the probabilities of the outside shell states, for example, in the ${}^{12}\text{C}$ nucleus, similarly to the case with the ${}^4\text{He}$ nucleus, we must bear in mind that the nucleus spin of ${}^{12}\text{C}$ can take the values $0 \leq S \leq 6$, the total orbital momentum of the nucleons of ${}^{12}\text{C}$ can be $0 \leq L \leq 6$, and the orbital momenta of separate nucleons can take on any values, which are not forbidden by the Pauli principle. In other words, the ground state of the nucleus ${}^{12}\text{C}$ can be of the 1S_0 , 3P_0 , 5D_0 , 7F_0 , 9G_0 , ${}^{11}H_0$, or ${}^{13}I_0$ states. Nowadays, probability of these states is not held due to their extreme complication. However, the rough estimation of these probabilities can be achieved in the following way. Let us suppose the ${}^{12}\text{C}$ nucleus consist of three weakly bound α -clusters. The total momentum and parity conservation laws do not forbid, and the tensor part of NN interaction and $3NF$'s initiate states with the orbital momenta

larger than predicted by the nuclear shell model (NSM) [39, 40] in every cluster, in two clusters at one time or in all three clusters. In the result, the probability of these states in the ^{12}C can be higher than in the ^4He nucleus.

Using this supposition one can explain the row of the well-known nuclei properties. Particularly, it is possible to explain the significantly higher contribution of the spin-orbit interaction in the nuclei, than calculated in the NSM frames. Contribution of the spin-orbit interaction A nucleons in the potential energy nucleus can be assessed by the relation:

$$U_{SO} = -\lambda \left(\frac{\hbar}{Mc} \right)^2 \sum_{i=1}^A \frac{1}{r_i} \frac{\partial V_i}{\partial r_i} (\vec{l}_i \cdot \vec{s}_i), \quad (13)$$

where M is the nucleon mass, V_i is the spherically symmetrical potential, l is the orbital momentum, s is the spin of the nucleon. However, for the agreement of the experimental data into the expression (13) was put a constant, which is $\lambda \sim 10$.

The appearance of the fitting constant λ can be partially explained as follows. Let k -number of the nucleons, with the orbital momenta in accordance with the NSM, and other $A-k$ nucleons have orbital momenta bigger than it is predicted by the NSM. Then the expression (13) can be refined as:

$$U_{SO} = - \left(\frac{\hbar}{Mc} \right)^2 \left[\sum_{i=1}^k \frac{1}{r_i} \frac{\partial V_i}{\partial r_i} P(l_i^{sh}) (\vec{l}_i^{sh} \cdot \vec{s}_i) + \sum_{i=k+1}^A \frac{1}{r_i} \frac{\partial V_i}{\partial r_i} P(l_i > l_i^{sh}) (\vec{l}_i \cdot \vec{s}_i) \right], \quad (14)$$

where $P(l_i)$ is the probability for the i -th nucleon to have the orbital momentum l_i . The sum of probabilities is $\sum_{i=1}^A P(l_i) = 1$. Thus, in the case of the lightest nuclei second summing of the expression (14) leads to the small but not equal zero impact of spin-orbit interaction to the potential energy of the nucleus. In medium and heavy nuclei nucleons are situated, generally, in $l > l^{sh}$ states. In other words, the tensor part of NN potential and $3N$ forces push the nucleons outside of nuclear shells, with the rise of atomic number the role of this effects is rising at that. The second summing, which is not predicted by NSM, can give a significant additional contribution to potential energy of a nucleus.

In particular, calculations [41, 42], made on the basis of the Woods-Saxon potential, can give the overestimation of the protons number Z for the position of the island of stability of the superheavy nuclei. In the frames of semiempirical shell models [43] at the extrapolation of fitting expressions for the area of the heavy nuclei to the area of the superheavy nuclei, apparently, the according corrections should be also counted

5 Conclusions

Modern methods of the decision of a many-nucleon problem make it possible to calculate the characteristics of this nucleus to an accuracy, which is determined by the accuracy the measurement of NN potential, and $3NF, s$ forces. In this connection the ^4He nucleus is an ideal laboratory for investigating the properties of these forces. The measurement of total cross-sections for the electromagnetic transitions with spin $S=1$ in the final state of the particle system in $^4\text{He}(\gamma, p)^3\text{H}$ and $^4\text{He}(\gamma, n)^3\text{He}$ reactions, and, in addition to data about radiative deuteron-deuteron capture, can give new information about of the structure of ^4He nucleus.

The states with non-zero orbital momenta of the nucleons of the lightest nuclei are the manifestation of the properties of inter-nucleonic forces and, consequently, such effects should be observed in all nuclei and in all their excited states without any exception. One can propose, that the tensor part of NN potential and $3N$ forces push the nucleons outside of nuclear shells, with the rise of atomic number the role of this effects is rising at that. This can lead to the additional contribution of the spin-orbital interaction to the potential energy of the nucleus. In particular, calculations, made on the basis of the Woods-Saxon potential, can give the overestimation of the protons number Z for the position of the "stability island" of the superheavy nuclei.

Author gives the gratitude to Yu.P. Stepanovsky for important advice and discussion over the article material, and to A.V. Shebeko for the sequence of critical remarks.

References

- [1] R.W.Woods and D.S.Saxon, Phys. Rev. **95**, 577 (1954).
- [2] R.B. Wiringa, V.G.J. Stoks, and R. Schiavilla, Phys. Rev. **C 51**, 38 (1995).
- [3] R. Machleidt, Phys. Rev. **C 63**, 024001 (2001). A. Deltuva, R. Machleidt, and P.U. Sauer, Phys. Rev. **C 68**, 024005 (2003).
- [4] L.D. Faddeev, Zh. Eksp. Theor. Fiz. **39**, 1459 (1960).
- [5] O. Yakubovsky, Sov. J. Nucl. Phys. **5**, 937 (1967).
- [6] B.S. Pudliner, V.R. Pandharipande, J. Carlson, S.C. Pieper, and R.B. Wiringa, Phys. Rev. **C 56**, 1720 (1997).
- [7] S.A. Coon, and J.L. Friar, Phys. Rev. **C 34**, 1060 (1986).
- [8] J.L. Friar, D. Huber, U. van Kolck, Phys. Rev. **C 59**, 53 (1999).
- [9] W. Gloeckle, and H. Kamada, Nucl. Phys. **A560**, 541 (1993).
- [10] W. Gloeckle, and H. Kamada, Phys. Rev. Lett. **C 71**, N7 (1993)
- [11] A. Nogga, H. Kamada, W. Gloeckle, and B.R. Barrett, Phys. Rev. **C 65**, 054003 (2002).
- [12] A. Nogga, H. Kamada, and W. Gloeckle, Phys. Rev. Lett. **85**, N5, 944 (2000).
- [13] W. Gloeckle, H. Witala, D. Huber, H. Kamada, and J. Golak, Phys. Rep. **274**, 107 (1996).
- [14] H. Witala, W. Gloeckle, Eur. Phys. J. **A 37**, N1 (2008).
- [15] S. Bacca, N. Barnea, W. Leidemann, and G. Orlandini, Phys.Rev. **C80**, 064001 (2009). e-Print: arXiv:0909.4810 [nucl-th].
- [16] A. Kievsky, M. Viviani, L. Girlanda, and L.E. Marcucci, Phys.Rev. **C 81**, 044003 (2010).
- [17] M. Trini, Ph.D. thesis, University of Erlangen-Nurnberg (2006).
- [18] H. Kamada, A. Nogga, W. Gloeckle, E. Hiyama *et al.*, Phys. Rev. **C64**, 044001 (2001).

- [19] K. Sekiguchi, H. Sakai, H. Witala, W. Gloeckle *et al.*, Phys. Rev. **C 79**, 054008 (2009).
- [20] E.J. Brach, O. Hausser, B. Larson, A. Rachav *et al.* Rhys. Rev. **C47**, 2064 (1993).
- [21] Q. Ye, G. Laskaris, W. Chen, H. Gao *et al.*, Eur. Phys. J. **A44**, 55 (2010).
- [22] X. Zong, Ph.D. thesis, Department of Physics Duke University (2010).
- [23] D.R. Entem and R. Machleidt, Phys. Rev. **C 68**, 041001 (R) (2003).
- [24] D. Rozpedzik, J. Golak, R. Skibinski *et al.*, Acta Phys.Polon. **B37**, 2889 (2006). e-Print: nucl-th/0606017.
- [25] V.N. Gur'ev, Preprint KhIPT 71-15 (1971)(in Russian).
- [26] J.D. Irish, R.G. Johnson, B.L. Berman, B.J. Thomas, K.G. McNeill, and J.W. Jury, Can. J. Phys. **53**, 802 (1976).
- [27] Yu.P. Lyakhno, I.V. Dogyust, E.S. Gorbenko, V.Yu. Lyakhno, S.S. Zub, Nucl. Pys. **A 781**, 306 (2007).
- [28] B.T. Murdoch, D.K. Hasell, A.M. Sourkes, W.T.H.van Oers, P.J.T. Verheijen, and R.E. Brown, Phys.Rev., **C 29**, 2001 (1984).
- [29] Yu.P. Lyakhno, V.I. Voloshchuk, V.B. Ganenko *et al.*, Phys. of At. Nuclei **59**, 14 (1996).
- [30] E.A. Vinokurov, V.I. Voloshchuk, V.B. Ganenko *et al.*, Vopr. At. Nauki i Tekhn., ser. Nuclear physical studies (theory and experiment) 3(11), 79 (1990) (in Russian).
- [31] Yu.V. Vladimirov, V.I. Denyak, S.N. Dukov *et al.*, Preprint KhIPT, 89 (1989)(in Russian).
- [32] Yu.P. Mel'nik, A.V. Shebeko, Preprint KhIPT, 84-27 (1984)(in Russian).
- [33] A.A. Zayats, V.A. Zolenko, Yu.A. Kasatkin, S.N. Nagorny, Preprint KFTI 91-4, M.; (1991).
- [34] S.N. Nagorny, Yu.A. Kasatkin, V.A. Zolenko *et al.*, Yad. Fis. **53**, 365 (1991)(in Russian).
- [35] Yu.M. Arkatov, P.I. Vatset, V.I. Voloshscuk *et al.*, arXiv 1304.5398 [nucl-ex].
- [36] J.H. Eisenberg and W. Greiner. Excitation Mechanisms of the Nucleus, in books Nuclear Theory, vol. 2. Amsterdam, (1970).
- [37] W.K. Pitts, Phys. Rev. **C 46**, 1215 (1992).
- [38] D.J. Wagenaar, N.R. Roberson, H.R. Weller and D.R. Tilley, Phys. Rev. **C 39**, 352 (1989).
- [39] M. Goeppert Mayer, J. Jensen. Elementary theory of nuclear shell structure. New York. USA: John Wiley and Sons. Inc.
- [40] T. Otsuka, T. Suzuki, R. Fujimoto *et al.*, Phys. Rev. Lett. **95**, 232502 (2005).
- [41] F.A. Gareev, B.N. Kalinkin, A. Sobiczewski, Phys. Lett. **22**, 500 (1966). R. Smolariczuk, Phys. Rev. **C 56**, 812 (1997).
- [42] F.A. Gareev, B.N. Kalinkin, A. Sobiczewski, Phys. Lett. **22**, 500 (1966).
- [43] R. Smolariczuk, Phys. Rev. **C 56**, 812 (1997).